Earth's Background Free Oscillations

Naoki Suda,* Kazunari Nawa, Yoshio Fukao

Earth's free oscillations were considered to be transient phenomena occurring after large earthquakes. An analysis of records of the IDA (International Deployment of Accelerometers) gravimeter network shows that Earth is freely oscillating at an observable level even in seismically inactive periods. The observed oscillations are the fundamental spheroidal modes at frequencies between 2 and 7 millihertz. Numerical modeling indicates that these incessant excitations cannot be explained by stacked effects of a large number of small earthquakes. The observed "background" free oscillations represent some unknown dynamic process of Earth.

Earth's free oscillations excited by large earthquakes have been analyzed for the past two decades to determine Earth's internal structure and earthquake mechanisms. Besides excitations caused by ordinary and slow earthquakes (*1*), weak and incessant excitations caused by random fluctuations in the fluid Earth or by unknown aseismic processes in the solid Earth are expected. Analysis of such signals, if they exist, should help to understand the dynamic processes affecting Earth. To search for possible weak and continuous signals of free oscillations, we created frequency-time spectrograms from low-frequency seismic records, which enabled us to examine the temporal variation of the power spectrum.

Seismic records from the IDA network (*2*) were suitable for such an analysis, because the IDA recording system is sensitive enough to low-frequency oscillations to observe the lowest frequency modes of the free oscillations (*3*), and there are high-quality records from 1976 to 1995. Each IDA station is equipped with a modified LaCoste-Romberg gravimeter with a 12-bit digital recording system. The digital unit of acceleration amplitude is on the order of 10^{-10} m/s^2.

We analyzed records for a 10-year period from 1986 to 1995 at station SUR (South Africa), which is known as one of the quietest seismic stations (*4*). The whole record is divided into 3-day periods with a time lag of 1 day. We tapered each record with a normalized Hanning taper and then calculated its power spectral density (PSD) with a fast Fourier transformation. A correction was made for the effect of filtering in the recording system (*5, 6*). The successive PSDs were then pasted up along a time axis to obtain the spectrogram.

Large earthquakes excite many modes of the free oscillations, so they can easily be identified as horizontal lines on a spectrogram (Fig. 1). In general, the rapid decay of these modes makes it difficult to identify them as vertical lines. Instead, we observed less distinctive but continuous vertical lines at frequencies between 3 and 6 mHz (Fig. 1). They are persistent through the 10-year period of the analysis, and their intensities are not affected by the occurrence of large earthquakes. Frequencies of the vertical lines agree with the eigenfrequencies of the fundamental spheroidal modes. Such an agreement indicates that the observed vertical lines represent the fundamental spheroidal modes of Earth's free oscillations that are continually excited at an observable level.

We also analyzed the records for stations BDF (Brazil), CMO (Alaska), HAL (Canada), KIP (Hawaii), NNA (Peru), PFO (California), RAR (Tonga), as well as SUR and TWO (Australia) from 1977 to 1980 as well as the SPA (the South Pole) records from 1993 to 1994. Spectrograms for all the stations except RAR, a noisy station (*7, 8*), also show the vertical lines corresponding to the fundamental spheroidal modes, although not all of them show such a clear signature like SUR because of the lower signal-to-noise ratios at the other stations. These oscillations have been detected in the Northern and Southern hemispheres wherever the ground noise is low, a feature expected from the global nature of Earth's free oscillations.

The most likely source of the observed oscillations is earthquakes. To determine whether earthquakes could account for the oscillations, we synthesized the spectrogram for the same period as in Fig. 1, assuming that earthquakes are the only sources for the oscillations. We adopted PREM (*9*) as the Earth model and used earthquake parameters given by the Harvard Centroid Moment Tensor (CMT) catalog (*10*). For each earthquake listed in the catalog, we calculated a synthetic seismogram by summing all the normal modes at frequencies below 10 mHz (*11*). The data length is varied according to the seismic moment with a minimum of 3 days and a maximum of 50 days. We merged all of the individual synthetic seismograms to create a 10-year-long synthetic seismogram.

A large number of smaller earthquakes not included in the catalog may be responsible for the weak but incessant excitation of the free oscillations. We examined this possibility by adding the effect of smaller earthquakes to the above synthetic seismogram. We note that in the CMT catalog, earthquakes with seismic moments (M_o) greater than $10^{17.2}$ N·m (moment magnitude M_w = 5.4) approximately follow the Gutenberg-Richter (G-R) magnitude-frequency relation. Assuming that this G-R relation can be extended to smaller earthquakes, and assuming that their random occurrence is described by a Poisson's distribution, we generated about 2000 earthquakes per year with $M_o > 10^{16}$ N·m (M_w = 4.6), for each of which the seismogram is randomly chosen from precalculated synthetic seismograms for real earthquakes, and only its amplitude is adjusted according to the seismic moment.

In general, a digital recording system does not sample a signal smaller than a digital unit if no noise exists. Addition of noise with an appropriate intensity, however, enables the signal to be sampled so that we can detect it. To include this effect, known as the stochastic resonance (*12*), we added synthetic random noise, the PSD of which is shaped similar to the observed one in a quiet period of observation, and digitized with a unit of 10^{-10} m/s^2. The synthetic noise PSD is flat at frequencies above 4 mHz and increases with decreasing frequency. The synthetic seismogram was then processed to obtain a spectrogram (Fig. 2). Although the synthetic spectrogram includes the effect of small earthquakes in a magnitude range between 4.6 and 5.4, there is practically no difference between the synthetic spectrograms with and without this effect, as expected from the theoretical consideration (*13*). This implies that if the effect of even smaller earthquakes (M_w < 4.6) were included, the resultant spectrogram would not change. The observed spectrogram (Fig. 1) shows the horizontal lines due to the excitation of modes by large earthquakes, which are well reproduced in the synthetic spectrogram (Fig. 2). In particular, the PSD values of the modes excited by large earthquakes are in quantitative agreement between the observed and synthetic spectrograms. The synthetic spectrogram shows vertical lines which correspond to the fundamental spheroidal modes, though very weak and less continuous relative to the observed ones. These vertical

N. Suda and K. Nawa, Department of Earth and Planetary Sciences, Nagoya University, Nagoya, Japan.
Y. Fukao, Earthquake Research Institute, University of Tokyo, Tokyo, Japan.

*To whom correspondence should be addressed. E-mail: suda@eps.nagoya-u.ac.jp

lines can be interpreted as a consequence of stochastic resonance arising from the noise addition and subsequent digitization. If the signal was initially digitized and then the noise was added, such vertical lines would not appear.

A more quantitative comparison may be made as follows. Referring to the Harvard CMT catalog, we excluded time intervals that contained the day of and the day immediately following earthquakes with $M_o > 10^{17.7}$ N·m (M_w = 5.7). The remaining intervals represent the seismically inactive periods. The PSDs for these periods were stacked to obtain an averaged PSD. The observed PSD (Fig. 3A) exhibits distinct spectral peaks at frequencies between 2 and 7 mHz, which are in a one-to-one correspondence with the fundamental spheroidal modes. We calculated the 90% confidence interval of the PSD, using a jackknife method (*14*). The averaged width of the confidence interval at frequencies between 2 and 7 mHz is 0.77 dB or 0.32×10^{-18} m^2/s^3 for the spectral peaks with an average intensity of 1.8×10^{-18} m^2/s^3. The peaks at frequencies between 3 and 6 mHz appear as vertical lines on the observed spectrogram. At frequencies above 7 mHz, the effect of mode coupling due to lateral heterogeneity in the crust and mantle prevents the modes from appearing as isolated spectral peaks. At frequencies below 2 mHz, the instrumental noise and noise due to atmospheric gravitational attraction obscure the spectral peaks (*7*, *15*).

The synthetic PSD (Fig. 3B), on the other hand, does not show such clear spectral peaks as the observed PSD. Reduction of the synthetic noise level does not enhance the spectral peaks. The focusing and defocusing effect due to lateral heterogeneity in mantle structure (*16*), which is not included in our modeling, will affect amplitudes of the free oscillations. However, the averaging procedure will minimize the effect of such amplitude variations. We conclude that the observed oscillations expressed as the vertical lines in the spectrogram cannot be explained by earthquakes. Slow earthquakes large and rapid enough to excite free oscillations but too slow to generate high-frequency seismic waves have been reported to occur several times a year (*1*). The moment magnitudes of these earthquakes are, however, in a range from 6 to 7, and even if smaller slow earthquakes are assumed to occur according to the G-R relation, they altogether are not powerful enough to account for the observed oscillations.

The dominance of fundamental modes suggests that the source of background free oscillations exists near Earth's surface. A possible source is random atmospheric loading. In a model recently proposed (*17*) the buoyant air warmed by absorption of infrared radiation from Earth's surface drives atmospheric turbulence which is random at scales beyond a characteristic length of the pressure scale height. The thermal energy carried upward by this turbulence is eventually released back to outer space. An analysis of the balance between this energy and incoming solar energy allows us to obtain an expression for frequency-dependent pressure disturbance. This disturbance inputs energy to the solid Earth and excites free oscillations, which are eventually dissipated as heat. A budgetary consideration on the input and dissipated energy yields a rough estimate of acceleration amplitudes, which are flat at a few nanogalileos (10^{-11} m/s^2) over the normal mode band. The level of the observed spectral peaks is more or less flat with the equivalent acceleration amplitude of nanogalileo level at frequencies above 4 mHz (Fig. 3A), thus supporting the atmospheric origin hypothesis. Such spectral flatness would not be expected if the modes were excited by earthquakes. An

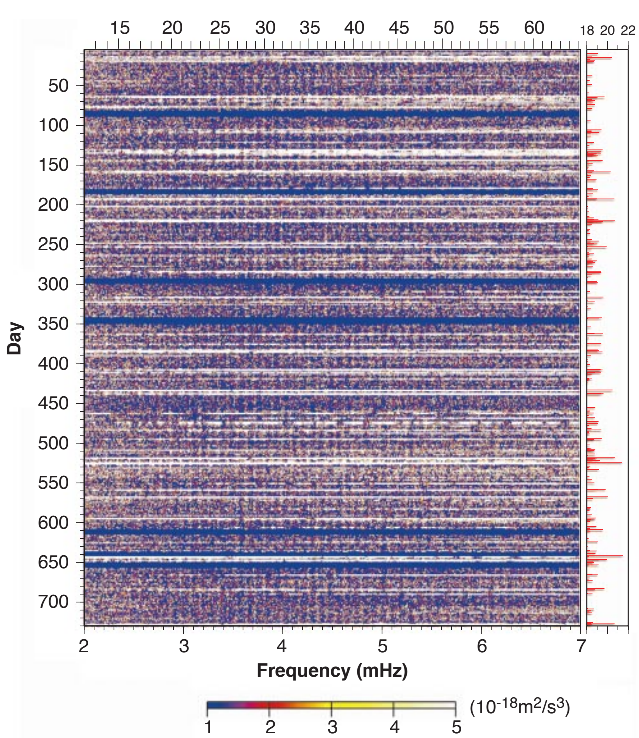

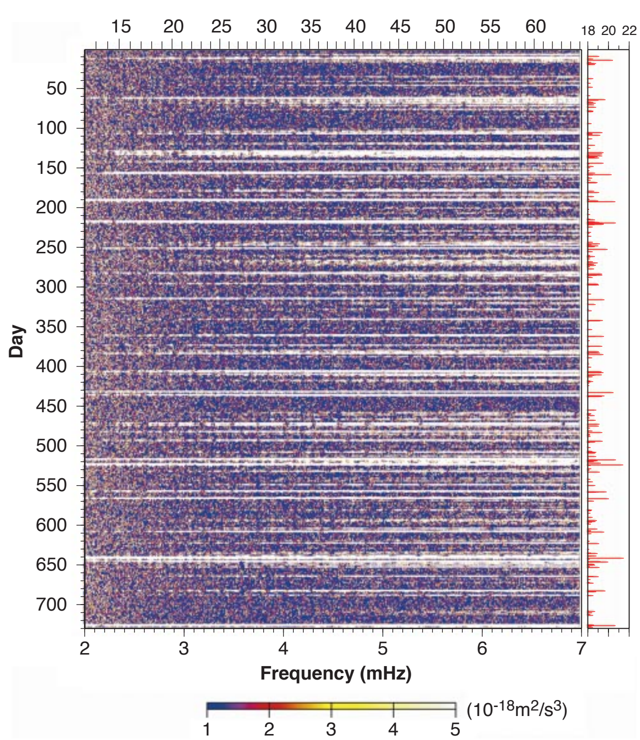

Fig. 1 (**left**). Spectrogram for the observed data for the period from 1993 to 1994 at station SUR. There are several null-valued intervals due to data losses. Tick marks and numbers at the top indicate eigenfrequencies of the fundamental spheroidal modes and mode angular orders, respectively. Horizontal bars at the right indicate seismic moments (in newton-meters) of large earthquakes in a logarithmic scale. Besides excitations of the modes by large earthquakes that are expressed as horizontal lines, weak and incessant excitations of the fundamental spheroidal modes are expressed as weak, continuous vertical lines. **Fig. 2** (**right**). Spectrogram is the same as Fig. 1, but for the synthetic data. The spectrogram shows vertical lines, though very weak and less continuous relative to the observed ones, which correspond to the fundamental spheroidal modes. The difference of line intensities indicates that the vertical lines seen on Fig. 1 are only in part due to the earthquake activity.

earthquake can be modeled as a double couple force acting stepwise in time and pointwise in space. Such a force near Earth's surface excites fundamental spheroidal modes whose amplitudes increase with increasing frequency.

Other possibilities, including undetected aseismic events at oceanic ridges and deep-sea trenches, cannot be excluded. Analyses of horizontal component records are crucial to understanding the excitation mechanism of background free oscillations, because random atmospheric or oceanic loading will hardly excite the toroidal modes, which is likely to be excited efficiently if the source was within the solid Earth. If only the spheroidal modes were observed on the horizontal component records, then the atmospheric origin of our observed oscillations would be favored. Unfortunately, it is difficult to detect weak signals at a required level from the horizontal component records of recent global seismic networks because the records usually suffer from large amounts of low-frequency noise (*18*).

We recently analyzed the records of a superconducting gravimeter at Syowa Station, Antarctica, and obtained a spectrogram showing the vertical lines at frequencies mostly corresponding to the fundamental spheroidal modes (*19*). The lines in the superconducting gravimeter spectrogram show the following characteristics: (i) They are visible even at frequencies down to 0.3 mHz, (ii) their intensity is seasonally varying, (iii) they have high intensity at frequencies between 3 and 4 mHz, and (iv) other lines that do not correspond to seismic normal modes are present. We find no such characteristics in the IDA spectrograms. The origin of these differences is now under consideration.

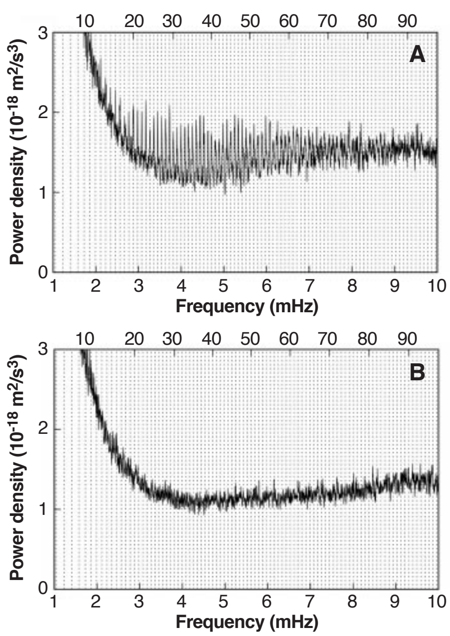

Fig. 3. Comparison of the averaged power spectral density at SUR between (**A**) the observed and (**B**) synthetic spectrograms for the seismically inactive periods, which are 437 days (12% of the total record) selected from the 10-year period. Vertical dotted lines indicate eigenfrequencies of the fundamental spheroidal modes; numbers at top indicate mode angular orders. In (A), clear spectral peaks can be seen, which are observed as the vertical lines in Fig. 1. No such clear peaks are seen in (B).

REFERENCES AND NOTES

1. G. C. Beroza and T. Jordan, *J. Geophys. Res.* **95**, 2485 (1990).
2. D. C. Agnew *et al.*, *Eos* **57**, 180 (1976).
3. R. Buland, J. Berger, F. Gilbert, *Nature* **277**, 358 (1979).
4. *Federation of Digital Seismograph Networks Station Book* (Incorporated Research Institutions for Seismology, Washington, DC, 1994).
5. D. C. Agnew *et al.*, *Eos* **67**, 203 (1986).
6. The IDA project team provides computer routines of the system response for calibrating amplitude and phase of seismic records. Uncertainty in the amplitude response is less than several percent, which does not affect our results.
7. D. C. Agnew and J. Berger, *J. Geophys. Res.* **83**, 5420 (1978).
8. Low-frequency noise at RAR is an order of magnitude larger than that at an average station.
9. A. M. Dziewonski and D. L. Anderson, *Phys. Earth Planet. Inter.* **25**, 297 (1981).
10. A. M. Dziewonski, G. Ekström, M. P. Salganik, *ibid.* **91**, 187 (1995).
11. F. Gilbert and A. M. Dziewonski, *Philos. Trans. R. Soc. London Ser. A*, **278**, 187 (1975).
12. A. R. Bulsara and L. Gammaitoni, *Phys. Today* **49**, 39 (1996).
13. Mode amplitude $A(M_o)$ is proportional to the seismic moment M_o if the attenuation effect is ignored. Let the number of earthquakes with seismic moments in a range from M_o to $M_o + dM_o$ be $n(M_o)dM_o$. According to the G-R relation, $n(M_o)$ is proportional to $M_o^{-5/3}$ if the *b* value is unity. Random occurrence of earthquakes with moments up to M_o contributes to the resultant amplitude as $[\int_0^{M_o} A(M_o)^2 n(M_o) dM_o]^{1/2}$, which is proportional to $M_o^{2/3}$. This means that the contribution of earthquakes with magnitudes up to M_w is only one-tenth of that of earthquakes with magnitudes up to $M_w + 1$.
14. D. J. Thomson and A. D. Chave, in *Advances in Spectrum Analysis and Array Processing*, S. Haykin, Ed. (Prentice-Hall, Englewood Cliffs, NJ, 1991), pp. 58–113.
15. R. J. Warburton and J. M. Goodkind, *Geophys. J. R. Astron. Soc.* **48**, 281 (1977).
16. T. Lay and H. Kanamori, *J. Geophys. Res.* **90**, 605 (1985).
17. N. Kobayashi, paper presented at the Fall Meeting of the Japanese Society for Planetary Sciences, Fukuoka, Japan, 4 October 1996.
18. G. G. Sorrells, *Geophys. J. R. Astron. Soc.* **26**, 71 (1971).
19. K. Nawa *et al.*, *Earth Planets Space*, **50**, 3 (1998).

18 November 1997; accepted 17 February 1998

Formation of a Magmatic-Hydrothermal Ore Deposit: Insights with LA-ICP-MS Analysis of Fluid Inclusions

Andreas Audétat,* Detlef Günther, Christoph A. Heinrich

The physical and chemical mechanism of ore precipitation in the Yankee Lode tin deposit (Mole Granite, Australia) was quantified by direct trace-element microanalysis of fluid inclusions. Laser ablation–inductively coupled plasma–mass spectrometry (LA-ICP-MS) was used to measure element concentrations in a series of fluid inclusions representing the fluid before, during, and after the deposition of cassiterite (SnO_2). Tin precipitation was driven by mixing of hot magmatic brine with cooler meteoric water. At the same time, a separate magmatic vapor phase selectively transported copper and boron into the liquid mixture.

Magmatic-hydrothermal ore deposits are a main source of Cu, W, Sn, Mo, and Au (*1*). They result from a sequence of complex geological processes beginning with the generation of hydrous silicate magmas, followed by their crystallization, the separation of volatile-rich magmatic fluids, and finally, the precipitation of ore minerals in veins or replacement deposits (*2*). A quantitative understanding of the latter two stages has been limited by a lack of information about trace-element concentrations in evolving hydrothermal fluids. Two specific questions depend on such data: (i) the role of magmatic brine-vapor separation in selective metal transport and (ii) the chemical reactions and relative importance of different physical processes leading to ore-mineral precipitation.

Experimental laboratory studies (*3, 4*) and surface sampling of fluids from active geothermal areas and volcanic gas discharge sites have provided important information on the concentrations and solubilities of metals in hydrothermal fluids. Direct information about the nature of fluids at several kilometers depth and at temperatures as

Institute for Isotope Geology and Mineral Resources, ETH Zentrum NO, CH-8092 Zürich, Switzerland.

*To whom correspondence should be addressed. E-mail: audetat@erdw.ethz.ch